Virus Host Recognition

DOI: 10.1002/anie.201105719

Molecular Details of the Recognition of Blood Group Antigens by a Human Norovirus as Determined by STD NMR Spectroscopy**

*Brigitte Fiege, Christoph Rademacher, Jonathan Cartmell, Pavel I. Kitov, Francisco Parra, and Thomas Peters**

Noroviruses from the family of *Caliciviridae* are the major cause of nonbacterial acute gastroenteritis worldwide, imposing a substantial burden on health care systems.[1] Currently, no direct treatment or vaccination strategy is available. The limited availability of animal models and cell culture systems[2] has drawn the main focus towards research with virus-like particles (VLPs).[3] In this study, the binding of VLPs of a GII.4 norovirus strain to host attachment factors has been investigated by NMR spectroscopy. These factors are human blood group antigens (HBGAs), and therefore virus attachment is based on specific carbohydrate–protein interactions.[4] It has been shown in prior studies that native viruses[5] and VLPs[6] are ideal targets for saturation transfer difference (STD) NMR experiments.[7] Therefore, we have utilized STD NMR experiments in conjunction with transfer NOESY experiments[8] to elucidate the binding epitopes and bioactive conformations of synthetic HBGA fragments. Understanding interactions between the virus and the host cell at atomic detail is of fundamental importance for the development of entry inhibitors.

In the first step, we subjected synthetic HBGA saccharides and fragments thereof to STD NMR experiments in the presence of norovirus (NV) VLPs. These experiments provided overall binding patterns that were compared to those of two other caliciviruses (Table 1), that is, to rabbit hemorrhagic disease virus (RHDV)[6b] and bovine norovirus (BNV).[6d] In the context of this work, "binding" means STD signals were observed and "nonbinding" indicates no STD signals were observed. As apparent from Table 1 both NV and RHDV require L-fucose moieties as minimal recognition elements, whereas BNV recognizes the α-D-Gal-(1,3)-α-D-Gal epitope. Comparison of the L-fucose specificities of NV and RHDV reveals subtle differences. The observation of STD signals for L-galactose (**22**) in the presence of RHDV VLPs but not in the presence of NV VLPs demonstrates that RHDV tolerates replacement of a hydrogen at C6 of L-fucose (**1**, **2**) by a hydroxy group. At this point, it is instructive to align these observations with crystal structure data available for the related NV strain VA387 (see Figure S9 in the Supporting Information for sequence alignment) in complex with B antigen trisaccharide.[9] In this structure, the methyl group of the L-fucose residue is buried in a hydrophobic pocket formed by Y443 and stabilized by H395 at the dimer interface (Figure S1 in the Supporting Information). The C6 hydroxy group of L-galactose likely disrupts this hydrophobic interaction, which explains the absence of STD effects. The amino acids recognizing the L-fucose are found to be strictly conserved across a broad range of GII.4 strains,[10] suggesting that this binding pocket and its corresponding ligand L-fucose are ideal targets for the design of entry inhibitors against GII.4 norovirus infections.

STD NMR experiments furnish the binding epitopes of HBGAs listed in Table 1. Two representative epitopes of A antigen trisaccharide **4** (ABH-antigen) and of sialyl Lewis^x (sLe^x) **14** are shown in Figure 1. All other binding epitopes are compiled in Figure S3 in the Supporting Information. In each case, L-fucose receives the highest fraction of saturation. This is in excellent agreement with crystal structure data of VA387 soaked with the A and B antigen trisaccharides[9] where L-fucose has been found to make many close contacts with amino acids in the binding pocket. The α-D-GalNAc and the α-D-Gal residue of A and B antigen trisaccharides **4** and **5**, respectively, also receive significant fractions of saturation. Both moieties make several contacts with the protein in the crystal structure.[9]

For H antigen type 1, 2, and 6 trisaccharides (**6**, **7**, and **8**) significant saturation transfer to the L-fucose moiety and only minor transfer to the corresponding backbone disaccharides is observed. The non-fucosylated precursor disaccharides **23**, **24**, and **26** give no STD response.

Comparison of binding epitopes of HBGA fragments for NV and RHDV[6b] reveals a preference for type 2 structures and even weak binding to the non-fucosylated type 2 pre-

[*] B. Fiege, Dr. C. Rademacher,[+] Prof. Dr. T. Peters
Center of Structural and Cell Biology in Medicine
Institute of Chemistry, University of Lübeck
Ratzeburger Allee 160, 23562 Lübeck (Germany)
E-mail: thomas.peters@chemie.uni-luebeck.de
J. Cartmell, Dr. P. I. Kitov
Department of Chemistry, University of Alberta
Edmonton, Alberta T6G 2G2 (Canada)
Prof. Dr. F. Parra
Instituto Universitario de Biotecnología de Asturias
Departamento de Bioquímica y Biología Molecular
Universidad de Oviedo, 33006 Oviedo (Spain)
[+] Present address:
Department of Chemical Physiology and Molecular Biology
The Scripps Research Institute, La Jolla, CA 92037 (USA)

[**] T.P. acknowledges the DFG for grant Pe494/8-1 and for grants HBFG 101/192-1 and ME 1830/1. B.F. thanks the Studienstiftung des deutschen Volkes for a stipend and C.R. thanks the Verband der Chemischen Industrie (VCI) for a stipend. F.P. thanks the Spanish Ministerio de Ciencia e Innovación for grant BIO2009-07535 and the European Union FEDER program for support. The work of P.I.K. was supported by the Alberta Ingenuity Centre for Carbohydrate Science and the Natural Science and Engineering Research Council of Canada. STD = saturation transfer difference.

Supporting information for this article is available on the WWW under http://dx.doi.org/10.1002/anie.201105719.

Table 1: HBGA fragments classified as binders or nonbinders according to the presence (+) or absence (−) of STD signals.[a]

Structure (name)	NV[b]	RHDV[c]	BNV[d]
α/β-L-Fuc (**1**)	+	n.d.	n.d.
α-L-Fuc-(1,*O*)-CH_3 (**2**)	+	+	n.d.
α-L-Fuc-(1,2)-β-D-Gal (H antigen disaccharide) (**3**)	+	+	n.d.
α-L-Fuc-(1,2)-[α-D-GalNAc-(1,3)]-β-D-Gal (A antigen trisaccharide) (**4**)	+	n.d.	n.d.
α-L-Fuc-(1,2)-[α-D-Gal-(1,3)]-β-D-Gal (B antigen trisaccharide) (**5**)	+	+	−
α-L-Fuc-(1,2)-β-D-Gal-(1,3)-β-D-GlcNAc (H antigen type 1) (**6**)	+	-	n.d.
α-L-Fuc-(1,2)-β-D-Gal-(1,4)-β-D-GlcNAc (H antigen type 2) (**7**)	+	+	n.d.
α-L-Fuc-(1,2)-β-D-Gal-(1,4)-β-D-Glc (H antigen type 6) (**8**)	+	n.d.	n.d.
α-L-Fuc-(1,3)-β-D-GlcNAc-(1,*O*)-CH_3 (**9**)	+	n.d.	n.d.
β-D-Gal-(1,4)-[α-L-Fuc-(1,3)]-β-D-GlcNAc (Le^x) (**10**)	+	n.d.	−
β-D-Gal-(1,3)-[α-L-Fuc-(1,4)]-β-D-GlcNAc (Le^a) (**11**)	+	n.d.	n.d.
α-L-Fuc-(1,2)-β-D-Gal-(1,4)-[α-L-Fuc-(1,3)]-β-D-GlcNAc (Le^y) (**12**)	+	n.d.	n.d.
α-L-Fuc-(1,2)-β-D-Gal-(1,3)-[α-L-Fuc-(1,4)]-β-D-GlcNAc (Le^b) (**13**)	+	n.d.	n.d.
α-D-Neu5Ac-(2,3)-β-D-Gal-(1,4)-[α-L-Fuc-(1,3)]-β-D-GlcNAc (sLe^x) (**14**)	+	n.d.	n.d.
α-D-Neu5Ac-(2,3)-β-D-Gal-(1,3)-[α-L-Fuc-(1,4)]-β-D-GlcNAc (sLe^a) (**15**)	+	n.d.	n.d.
α/β-D-Gal (**16**)	−	−	−
β-D-Gal-(1,*O*)-CH_3	n.d	−	n.d.
α/β-D-GalNAc (**17**)	−	n.d.	n.d.
α/β-D-Glc (**18**)	−	−	n.d.
α/β-D-GlcNAc (**19**)	−	n.d.	n.d.
α/β-D-ManNAc (**20**)	−	n.d.	n.d.
α/β-D-Fuc (**21**)	−	−	n.d.
α/β-L-Gal (**22**)	−	+	n.d.
β-D-Gal-(1,3)-D-GlcNAc (type 1) (**23**)	−	−	−
β-D-Gal-(1,4)-D-GlcNAc (type 2) (**24**)	−	+	−
β-D-Gal-(1,3)-D-GalNAc (type 3) (**25**)	−	n.d.	n.d.
β-D-Gal-(1,4)-β-D-Glc-(1,*O*)-CH_3 (type 6) (**26**)	−	n.d.	n.d.
α-D-Neu5Ac-(2,3)-β-D-Gal-(1,4)-D-Glc (**27**)	−	n.d.	n.d.
α-D-Neu5Ac-(2,6)-β-D-Gal-(1,4)-D-Glc (**28**)	−	n.d.	n.d.
α-D-Gal-(1,3)-α-D-Gal-(1,*O*)-CH_3 (**29**)	−	n.d.	+

[a] As all ligands have at best high μM K_D values it is safe to assume that the absence of STD signals cannot reflect very tight binding and low off-rates. [b] NV = human norovirus Ast6139. [c] RHDV = rabbit hemorrhagic disease virus; data from Ref. [6b]. [d] BNV: bovine norovirus; data from Ref. [6d]. n.d. = not determined.

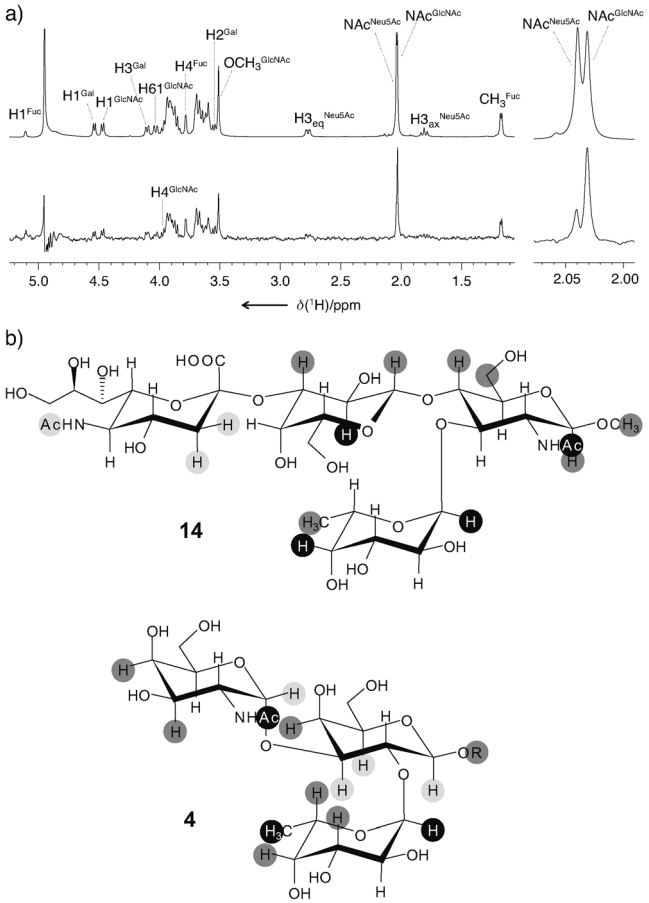

Figure 1. a) STD (bottom) and reference (top) ^{1}H NMR spectra (500 MHz, D_2O) of sLe^x **14** in the presence of NV VLPs measured at a saturation time of 0.5 s and a temperature of 282 K. b) Binding epitopes of sLe^x **14** (left) and A antigen trisaccharide **4** (right, R = $(CH_2)_7CH_3$). The relative STD effects (highest STD signal normalized to 100%) are illustrated by dark, medium. and light gray circles indicating strong (> 80%), medium (40–80%), and weak (< 40%) STD effects, respectively. Protons without a circle have not been analyzed owing to spectral overlap.

cursor disaccharide **24** in the case of RHDV. The binding epitope of H antigen type 2 trisaccharide **7** bound to RHDV further reflects significant saturation transfer also to the D-GlcNAc residue (Figure S4 in the Supporting Information). Obviously, RHDV discriminates host cell attachment factors also by interaction with the backbone region of HBGAs.

Sialylated glycans such as sLe^x are important molecules in cell signaling and are exploited by pathogens such as influenza virus,[11] rotavirus,[12] and polyomavirus[13] for host cell attachment and entry. Binding of GII.4 norovirus VLPs to sLe^x and to Lewis antigens has been previously demonstrated.[14] Recently, crystal structures have been obtained based on P-domain dimers of GII.4-, GII.9-, and GII.10-type noroviruses complexed with Lewis antigens[15] and in one case with sLe^x.[15c] In the case of the GII.9 structure with sLe^x in the binding pocket, very low electron density has been reported for the neuraminic acid residue, indicating disorder and hence flexibility of this residue. For the GII.4 strain studied here no such structural data are available yet, but STD NMR analysis provides binding epitopes of (sialyl) Lewis antigens bound to norovirus VLPs at atomic resolution. sLe^x (**14**) and sLe^a (**15**) as well as Le^x (**10**), Le^a (**11**), Le^y (**12**), and Le^b (**13**) show significant saturation transfer in the presence of NV, indicating that this strain is able to recognize fucosylated ligands regardless of the type of fucosidic linkage. Interestingly, for difucosylated Le^y **12** STD signals were observed for both L-fucose moieties, with slightly larger STD signals for the α-(1,2)-linked fucose. It is likely that the binding epitope represents an average of two binding modes where either of the fucose moieties may be accommodated in the binding

pocket. In case of Le^b **13** all fucose signals show severe overlap and could not be analyzed separately.

For Le^x and Le^a trisaccharides (**10** and **11**) the analysis of binding epitopes provides critical information on their relative orientation in the binding pocket. Le^x and Le^a can be superimposed in such a way that the fucose and galactose residues match while the GlcNAc pyranose ring is rotated by approximately 180°.[16] This places the *N*-acetyl group of Le^a in the position of the C6 hydroxymethyl group of Le^x and vice versa. The binding epitope of Le^x **10** shows a strong STD signal for its *N*-acetyl group, whereas in case of Le^a **11** almost no saturation transfer is observed to the *N*-acetyl group (Figure S5 in the Supporting Information), a difference even more pronounced for sLe^x and sLe^a (**14** and **15**). This result is in accordance with a positioning of Le^x and Le^a in the binding pocket such that fucose and galactose superimpose (see the discussion below).

Group epitope mapping for sLe^x and sLe^a suggests that the neuraminic acid residue has less contact with the protein surface than the other hexopyranoses. Only minor saturation transfer occurs to the *N*-acetyl side chain and H3$_{eq}^{Neu5Ac}$/H3$_{ax}^{Neu5Ac}$ (Figure 1 and Figures S3 and S6 in the Supporting Information). STD effects of the remaining protons could not be analyzed because of signal overlap. However, the absence of STD signals for 3′- and 6′-sialyllactose (**27** and **28**) is in accordance with a minor contribution of the neuraminic acid residue to NV binding.

On account of flexibility around the 2,3-glycosidic linkage, sLe^x can adopt two major conformational families in solution, of which usually only one is recognized by proteins such as E-selectin[17] and other lectins.[17c,18] To characterize the bioactive conformation of sLe^x we conducted transfer NOESY (trNOESY) experiments (Figure 2).

It was straightforward to identify transferred NOEs since under the conditions chosen, NOEs for free sLe^x were close to zero intensity (cf. Figure S7 in the Supporting Information). The experiments show that the Le^x trisaccharide backbone adopts a bioactive conformation that is identical with the major solution conformation termed "A" in Ref. [18]. This is deduced from interglycosidic trNOEs between H2^{Gal} and H5^{Fuc}/CH$_3^{Fuc}$ and between H1^{Fuc} and NAc^{GlcNAc}.

For the 2,3-glycosidic linkage of sLe^x one set of trNOE cross peaks unambiguously reflects the presence of conformers that are characterized by short distances (less than 3.5 Å) between H3^{Gal} and H3$_{eq}^{Neu5Ac}$/H3$_{ax}^{Neu5Ac}$, and between H3^{Gal} and H5^{Neu5Ac} (red arrows in Figure 2). In this conformation the 2,3-glycosidic linkage adopts dihedral angles ϕ of about −170° and ψ of about −10° (conformer "b" in Ref. [18]). The other major conformational state (conformer "a" in Ref. [18]) is characterized by dihedral angles ϕ of about −70° and ψ of about 0° and is usually experimentally verified by means of an NOE that is associated with the short distance between H3^{Gal} and H8^{Neu5Ac} (blue arrow in Figure 2). The corresponding cross peak is observed in the trNOESY spectra but it is weak (blue box in Figure 2). Simultaneous observation of both sets of mutually excluding interglycosidic trNOEs indicates that conformations "a" and "b" are both recognized by NV VLPs. The observations would also be in accordance with the flexibility of the neuraminic acid residue in the bound

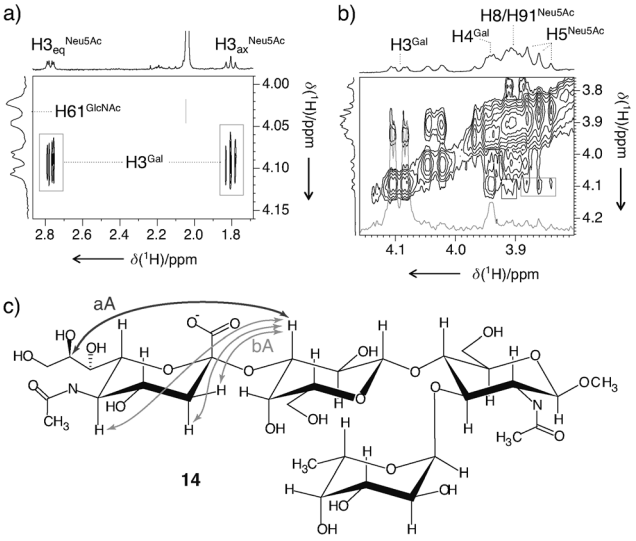

Figure 2. a,b) Portions of the trNOESY spectrum (500 MHz, D_2O) of 0.25 mM sLe^x **14** in the presence of 1.2 mg mL^{-1} NV VLPs; a 13:1 ratio of ligand to binding sites is observed if one assumes 180 binding sites per VLP. T = 298 K; mixing time: 250 ms. c) Interglycosidic trNOEs across the 2,3-glycosidic linkage between H3^{Gal} and H3$_{ax}^{Neu5Ac}$/H3$_{eq}^{Neu5Ac}$ and H5^{Neu5Ac} (light gray arrows corresponding to light gray boxes in (a,b)) and between H3^{Gal} and H8^{Neu5Ac} (dark gray arrow corresponding to the dark gray box in (b)).

state. The latter hypothesis is supported by recent X-ray diffraction data that display poor electron density for the neuraminic acid residue of sLe^x bound to a norovirus GII.9 P-domain dimer, indicating disorder of that residue in the bound state.[15c] Although the authors have fitted only conformation "a" to the electron density map we conclude that taken together with our experimental data—albeit on a different genotype (GII.4)—the neuraminic acid residue can adopt two conformations in the bound state as it also does in solution.

Since VLPs are rather large (about 10 MDa) very weak trNOE cross peaks can also arise from spin diffusion. This makes a quantification of trNOE data difficult. Therefore, we remain with a qualitative interpretation for now, according to which sLe^x bound to NV VLPs is characterized by a rigid Le^x backbone and a flexible 2,3-glycosidic linkage. This hypothesis is further substantiated by preliminary molecular dynamics (MD) simulations of sLe^x bound to NV.

The crystal structure of VA387[9] served as a model for the docking of HBGA ligands (Table 1). It has 96% sequence identity with the NV strain investigated and the amino acids involved in coordinating B antigen trisaccharide are fully conserved (Figure S9 in the Supporting Information). Structures of ABH and Lewis antigens were generated using Amber with Glycam parameters[19] and automated docking was achieved using Autodock Vina.[20] Only poses that matched the orientation of fucose in the crystal structure[9] and that were in accordance with the *exo* anomeric effect were considered as valid starting structures for MD simulation. Here, we report preliminary results for a 20 ns MD simulation with explicit water for sLe^x free and bound to NV (see the Supporting Information for details). The reader is also referred to a recent report on MD simulations for a

number of HBGA ligands excluding sLe^x, Le^x, and Le^a bound to NV.[21] Our MD simulation samples three conformational families in the bound state (Figure 3 and Figures S10 and S12

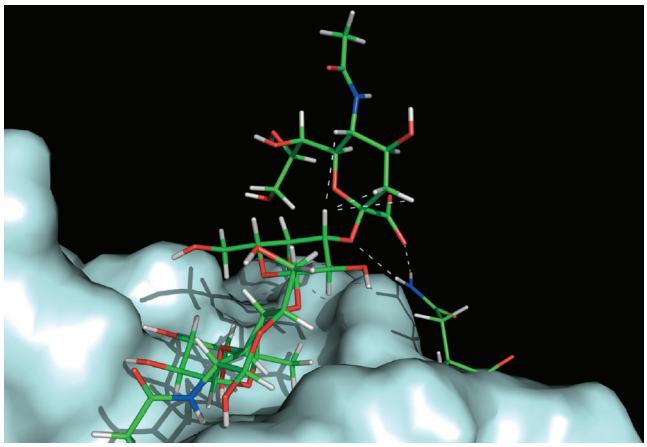

Figure 3. Snapshot of a 20 ns MD simulation of sLe^x **14** bound to NV. Water molecules are omitted for clarity. The MD simulation predicts that conformational family "b" becomes more abundant in the bound state owing to stabilization by a bidentate hydrogen bond between the glycosidic and the carboxylic oxygens of neuraminic acid and the side chain amide of N393 (the residue is shown as a wire protruding through the protein surface on the right). TrNOE-relevant distances between $H3^{Gal}$ and $H3_{ax}{}^{Neu5Ac}$, $H3_{eq}{}^{Neu5Ac}$, $H5^{Neu5Ac}$ are also marked. The figure was prepared with PyMOL (www.delanoscientific.com).

in the Supporting Information) substantiating the hypothesis that the 2,3-glycosidic linkage retains flexibility in the bound state. Two of these families correspond to the main minima "a" and "b" identified previously[18] (cf. Figure S12 in the Supporting Information). Interestingly, the simulation predicts that conformational family "b" is significantly more highly populated in the bound state than in the free state, which is in very good agreement with our trNOE data.

The docking poses of Le^x (**10**) and Le^a (**11**) were compared without any further MD simulations to qualitatively validate the observed differences in the saturation transfer towards the respective *N*-acetyl groups (Figures S3 and S5 in the Supporting Information). While the *N*-acetyl group of Le^x points towards the binding pocket and can potentially make contacts to A346, H347, C440, and S441, the *N*-acetyl group of Le^a could make only one contact to G392 (Figure S8 h,i in the Supporting Information). This correlates very well with the observation of much stronger STD effects for the *N*-acetyl group of Le^x (**10**) (cf. Figure S5).

To summarize, our experiments deliver for the first time a systematic overview of the structural requirements for norovirus attachment to host cell antigens (HBGAs) at atomic resolution. L-fucose has been identified as a minimal structural recognition element that is bound with remarkable specificity. Importantly, we suggest that the neuraminic acid residue of sLe^x (**14**) remains flexible in the bound state. Further experiments and MD simulations are underway to substantiate this hypothesis and to deliver more quantitative data. This study paves the way for further systematic studies into norovirus–host recognition and delivers valuable details for the design of entry inhibitors.

Experimental Section

A and B antigen trisaccharides with octyl spacers and the methyl glycoside derivative of the B antigen trisaccharide were enzymatically synthesized utilizing human blood group glycosyltransferases[22] and were kind gifts from Professor Monica Palcic (Carlsberg Laboratory). H antigen disaccharide and α-L-Fuc-(1,3)-β-D-GlcNAc-(1,*O*)-CH_3 were chemically synthesized in our institute (unpublished data). H antigen trisaccharides type 1 and type 2 were kind gifts from Professor Ole Hindsgaul (Carlsberg Laboratory). L-Fuc, α-L-Fuc-(1,*O*)-CH_3, D-Gal, β-D-Gal-(1,*O*)-CH_3, D-ManNAc, L-Gal, β-D-Gal-(1,4)-D-GlcNAc (type 2 precursor), β-D-Gal-(1,3)-D-GalNAc (type 3 precursor), and β-D-Gal-(1,4)-D-Glc (type 6 precursor) were purchased from Sigma. D-Fuc, β-D-Gal-(1,3)-D-GlcNAc (type 1 precursor), α-L-Fuc-(1,2)-β-D-Gal-(1,4)-D-Glc (H antigen trisaccharide type 6), 3′-sialyllactose, and 6′-sialyllactose were obtained from Dextra. D-GalNAc, D-Glc, and D-GlcNAc were obtained from Fluka, Merck, and Aldrich, respectively. Methyl glycosides of Le^x, Le^a, and sLe^x were purchased from Toronto Research Chemical. Tetrasaccharidic methyl glycosides of Le^b and Le^y were gifts from Professor Monica Palcic (Carlsberg Laboratory) and Professor Todd Lowary (University of Alberta), respectively. sLe^a with a carbamoyl spacer was a gift from Professor Beat Ernst (University of Basel). α-D-Gal-(1,3)-α-D-Gal-(1,*O*)-CH_3 was obtained from Calbiochem.

Details for the expression of VLPs and for the NMR experiments as well as for the docking studies are found in the Supporting Information.

Received: August 12, 2011
Published online: December 13, 2011

Keywords: bioactive conformations · blood group antigens · sialyl Lewis^x · NMR spectroscopy

[1] a) A. M. Hutson, R. L. Atmar, M. K. Estes, *Trends Microbiol.* **2004**, *12*, 279–287; b) A. Scipioni, A. Mauroy, J. Vinje, E. Thiry, *Vet. J.* **2008**, *178*, 32–45.

[2] a) E. Duizer, K. J. Schwab, F. H. Neill, R. L. Atmar, M. P. Koopmans, M. K. Estes, *J. Gen. Virol.* **2004**, *85*, 79–87; b) T. M. Straub, K. Honer zu Bentrup, P. Orosz-Coghlan, A. Dohnalkova, B. K. Mayer, R. A. Bartholomew, C. O. Valdez, C. J. Bruckner-Lea, C. P. Gerba, M. Abbaszadegan, C. A. Nickerson, *Emerging Infect. Dis.* **2007**, *13*, 396–403.

[3] X. Jiang, M. Wang, D. Y. Graham, M. K. Estes, *J. Virol.* **1992**, *66*, 6527–6532.

[4] a) V. Roldós, F. J. Canada, J. Jimenez-Barbero, *ChemBioChem* **2011**, *12*, 990–1005; b) M. L. DeMarco, R. J. Woods, *Glycobiology* **2008**, *18*, 426–440.

[5] A. J. Benie, R. Moser, E. Bauml, D. Blaas, T. Peters, *J. Am. Chem. Soc.* **2003**, *125*, 14–15.

[6] a) C. Rademacher, T. Peters, *Top. Curr. Chem.* **2008**, *273*, 183–202; b) C. Rademacher, N. R. Krishna, M. Palcic, F. Parra, T. Peters, *J. Am. Chem. Soc.* **2008**, *130*, 3669–3675; c) T. Haselhorst, J. M. Garcia, T. Islam, J. C. Lai, F. J. Rose, J. M. Nicholls, J. S. Peiris, M. von Itzstein, *Angew. Chem.* **2008**, *120*, 1936–1938; *Angew. Chem. Int. Ed.* **2008**, *47*, 1910–1912; d) M. Zakhour, N. Ruvoen-Clouet, A. Charpilienne, B. Langpap, D. Poncet, T. Peters, N. Bovin, J. Le Pendu, *PLoS Pathog.* **2009**, *5*, e1000504; e) T. Haselhorst, T. Fiebig, J. C. Dyason, F. E. Fleming, H. Blanchard, B. S. Coulson, M. von Itzstein, *Angew. Chem.* **2011**, *123*, 1087–1090; *Angew. Chem. Int. Ed.* **2011**, *50*, 1055–1058; f) C. Rademacher, J. Guiard, P. I. Kitov, B. Fiege, K. P. Dalton, F. Parra, D. R. Bundle, T. Peters, *Chem. Eur. J.* **2011**, *17*, 7442–7453.

[7] a) M. Mayer, B. Meyer, *Angew. Chem.* **1999**, *111*, 1902–1906; *Angew. Chem. Int. Ed.* **1999**, *38*, 1784–1788; b) M. Mayer, B.

Meyer, *J. Am. Chem. Soc.* **2001**, *123*, 6108 – 6117; c) B. Meyer, T. Peters, *Angew. Chem.* **2003**, *115*, 890 – 918; *Angew. Chem. Int. Ed.* **2003**, *42*, 864 – 890.
[8] G. M. Clore, A. M. Gronenborn, *J. Magn. Reson.* **1982**, *48*, 402 – 417.
[9] S. Cao, Z. Lou, M. Tan, Y. Chen, Y. Liu, Z. Zhang, X. C. Zhang, X. Jiang, X. Li, Z. Rao, *J. Virol.* **2007**, *81*, 5949 – 5957.
[10] L. C. Lindesmith, E. F. Donaldson, A. D. Lobue, J. L. Cannon, D. P. Zheng, J. Vinje, R. S. Baric, *PLoS Med.* **2008**, *5*, e31.
[11] S. J. Gamblin, J. J. Skehel, *J. Biol. Chem.* **2010**, *285*, 28403 – 28409.
[12] M. Baker, B. V. Prasad, *Curr. Top. Microbiol. Immunol.* **2010**, *343*, 121 – 148.
[13] U. Neu, T. Stehle, W. J. Atwood, *Virology* **2009**, *384*, 389 – 399.
[14] a) P. Huang, T. Farkas, W. Zhong, M. Tan, S. Thornton, A. L. Morrow, X. Jiang, *J. Virol.* **2005**, *79*, 6714 – 6722; b) G. E. Rydell, J. Nilsson, J. Rodriguez-Diaz, N. Ruvoen-Clouet, L. Svensson, J. Le Pendu, G. Larson, *Glycobiology* **2009**, *19*, 309 – 320; c) A. de Rougemont, N. Ruvoen-Clouet, B. Simon, M. Estienney, C. Elie-Caille, S. Aho, P. Pothier, J. Le Pendu, W. Boireau, G. Belliot, *J. Virol.* **2011**, *85*, 4057 – 4070.
[15] a) S. Shanker, J. M. Choi, B. Sankaran, R. L. Atmar, M. K. Estes, B. V. Prasad, *J. Virol.* **2011**, *85*, 8635 – 8645; b) G. S. Hansman, C. Biertumpfel, I. Georgiev, J. S. McLellan, L. Chen, T. Zhou, K. Katayama, P. D. Kwong, *J. Virol.* **2011**, *85*, 6687 – 6701; c) Y. Chen, M. Tan, M. Xia, N. Hao, X. C. Zhang, P. Huang, X. Jiang, X. Li, Z. Rao, *PLoS Pathog.* **2011**, *7*, e1002152.
[16] U. Spohr, O. Hindsgaul, R. U. Lemieux, *Can. J. Chem.* **1985**, *63*, 2644 – 2652.
[17] a) K. Scheffler, J. R. Brisson, R. Weisemann, J. L. Magnani, W. T. Wong, B. Ernst, T. Peters, *J. Biomol. NMR* **1997**, *9*, 423 – 436; b) K. Scheffler, B. Ernst, A. Katopodis, J. Magnani, W. T. Wang, R. Weisemann, T. Peters, *Angew. Chem.* **1995**, *107*, 2034 – 2037; *Angew. Chem. Int. Ed. Engl.* **1995**, *34*, 1841 – 1844; c) L. Poppe, G. S. Brown, J. S. Philo, P. V. Nikrad, B. H. Shah, *J. Am. Chem. Soc.* **1997**, *119*, 1727 – 1736; d) R. Harris, G. R. Kiddle, R. A. Field, M. J. Milton, B. Ernst, J. L. Magnani, S. W. Homans, *J. Am. Chem. Soc.* **1999**, *121*, 2546 – 2551.
[18] T. Haselhorst, T. Weimar, T. Peters, *J. Am. Chem. Soc.* **2001**, *123*, 10705 – 10714.
[19] K. N. Kirschner, A. B. Yongye, S. M. Tschampel, J. Gonzalez-Outeirino, C. R. Daniels, B. L. Foley, R. J. Woods, *J. Comput. Chem.* **2008**, *29*, 622 – 655.
[20] O. Trott, A. J. Olson, *J. Comput. Chem.* **2010**, *31*, 455 – 461.
[21] C. A. Koppisetty, W. Nasir, F. Strino, G. E. Rydell, G. Larson, P. G. Nyholm, *J. Comput.-Aided Mol. Des.* **2010**, *24*, 423 – 431.
[22] N. O. Seto, C. A. Compston, A. Szpacenko, M. M. Palcic, *Carbohydr. Res.* **2000**, *324*, 161 – 169.

